

Published in final edited form as:

*Future Neurol.* 2013 September ; 8(5): 583–597. doi:10.2217/fnl.13.37.

## Diffusion tensor imaging and related techniques in tuberous sclerosis complex: review and future directions

Jurriaan M Peters<sup>\*,‡,1,2</sup>, Maxime Taquet<sup>‡,2,3</sup>, Anna K Prohl<sup>1,2</sup>, Benoit Scherrer<sup>2</sup>, Agnies M van Eeghen<sup>4</sup>, Sanjay P Prabhu<sup>2</sup>, Mustafa Sahin<sup>1</sup>, and Simon K Warfield<sup>2</sup>

<sup>1</sup>Department of Neurology & the Division of Epilepsy & Clinical Neurophysiology, Boston Children's Hospital, 300 Longwood Avenue, Fegan 9, Boston, MA 02115, USA <sup>2</sup>Department of Radiology & the Computational Radiology Laboratory, Boston Children's Hospital, Boston, MA 02115, USA <sup>3</sup>ICTEAM Institute, Université catholique de Louvain, Place du Levant 2 bte L5.04.04, 1348 Louvain-La-Neuve, Belgium <sup>4</sup>Department of Neuroscience, ENCORE, Expertise Centre for Neurodevelopmental Disorders, Erasmus Medical Centre, PO Box 2040, 3000 CA Rotterdam, The Netherlands

### Abstract

In this article, the authors aim to introduce the nonradiologist to diffusion tensor imaging (DTI) and its applications to both clinical and research aspects of tuberous sclerosis complex. Tuberous sclerosis complex is a genetic neurocutaneous syndrome with variable and unpredictable neurological comorbidity that includes refractory epilepsy, intellectual disability, behavioral abnormalities and autism spectrum disorder. DTI is a method for modeling water diffusion in tissue and can noninvasively characterize microstructural properties of the brain. In tuberous sclerosis complex, DTI measures reflect well-known pathological changes. Clinically, DTI can assist with detecting the epileptogenic tuber. For research, DTI has a putative role in identifying potential disease biomarkers, as DTI abnormalities of the white matter are associated with neurocognitive morbidity including autism. If indeed DTI changes parallel phenotypical changes related to the investigational treatment of epilepsy, cognition and behavior with mTOR inhibitors, it will facilitate future clinical trials.

© 2013 Future Medicine Ltd

\*Author for correspondence: jurriaan.peters@childrens.harvard.edu.

‡Authors contributed equally.

**Financial & competing interests disclosure:** This work was supported in part by the NIH (grant numbers R01 RR021885, R01 LM010033, R03 EB008680 and UL1 RR025758 to SK Warfield; P20 RFA-NS-12-006 and 1U01NS082320-01 to M Sahin). In addition, JM Peters is supported by a Faculty Development Fellowship from the Eleanor and Miles Shore 50th Anniversary Fellowship Program for Scholars in Medicine, Boston Children's Hospital, Department of Neurology. M Taquet is supported by the Fonds de la Recherche Scientifique and the Belgian American Educational Foundation. M Sahin is supported by the Tuberous Sclerosis Alliance, Autism Speaks, John Merck Fund, Nancy Lurie Marks Family Foundation, Boston Children's Hospital, Translational Research Program and Boston Children's Hospital Intellectual and Developmental Disabilities Research Center (P30 HD18655). M Sahin is a consultant and site principal investigator for Novartis, Inc. and JM Peters is paid on a consultant basis for the Novartis EXIST-III trial: a three-arm, randomized, double-blind, placebo-controlled study of the efficacy and safety of two trough ranges of everolimus as adjunctive therapy in patients with tuberous sclerosis complex who have refractory partial-onset seizures. SK Warfield is a consultant for Siemens Medical Imaging, Inc. The authors have no other relevant affiliations or financial involvement with any organization or entity with a financial interest in or financial conflict with the subject matter or materials discussed in the manuscript apart from those disclosed.

No writing assistance was utilized in the production of this manuscript.

## Keywords

autism spectrum disorders; behavior; cognition; diffusion tensor imaging; epilepsy; MRI; mTOR serine–threonine kinases; tuberous sclerosis complex

Tuberous sclerosis complex (TSC) is a genetic neurocutaneous syndrome with an estimated incidence of one in 6000–10,000 [1,2]. Benign hamartomas, the hallmark of the disease, are found in multiple organ systems, including the brain, eyes, kidneys, lungs, skin and heart, and comprised nonmalignant and disorganized cells that often exhibit abnormal differentiation [3]. Inherited autosomal dominant mutations (<30%) and sporadic mutations (>70%) lead to inactivation of the tumor suppressor genes *TSC1* (on chromosome band 9q34) and *TSC2* (on chromosome band 16p13.3) and can be identified in 70–90% of patients who meet the clinical criteria of TSC [4,5]. TSC is diagnosed on the basis of major and minor clinical criteria, with three of the major criteria being based on neuroimaging findings [6]. In 2012, the International Tuberous Sclerosis Consensus updated the TSC diagnostic criteria from 1998; TSC can now be diagnosed via genetic testing if a pathogenic mutation is found [201].

Neurologically, TSC can manifest with developmental delay or intellectual disability, behavioral abnormalities, autism and seizures. Clinical presentation is highly variable and patients with a *TSC2* mutation typically present with a more severe neurological phenotype [7,8]. Epilepsy occurs in 80–90% of all patients, is often medically refractory, and any seizure type can be seen [1]. Autism spectrum disorders (ASD) occur in up to 50% of patients by the age of 5 years [9]. Close to 45% of patients have varying degrees of intellectual disabilities [5]. Neurological sequelae are particularly devastating in children as they appear early in life and affect neurological development, with long-term effects on academic and socioeconomic outcome.

Conventional anatomical MRI is routinely used for the detection and monitoring of major CNS lesions in both the diagnosis and management of TSC. Neuroimaging in patients under the age of 1 year with a clinical suspicion of TSC results in a definite diagnosis in 95% of cases [7]. While conventional MRI is highly sensitive, it only gives an impression of the extent of CNS involvement, and it does not provide much information on the neurobehavioral phenotype nor on epilepsy.

First, no robust MRI biomarker that correlates consistently with the clinical phenotype or neurological outcome has been identified. For example, the presence of tubers in the temporal lobe has been linked to the risk of autism [10], but other critical regions including the cerebellum have also been proposed [11–14]. Although associations have been made between total tuber load, epilepsy and cognitive function [12,14,15], age at seizure onset is the only consistent and independent determinant of cognitive function [16]. A high tuber load or tubers in specific locations are, therefore, neither necessary nor sufficient to predict (early) seizures, cognitive impairment or autism (Figure 1A & B) [16,17]. Inter- and intra-observer variability in determination of tuber burden may be reduced by automated tuber segmentation [16], but differences in magnet strengths, image acquisition specifics and quality form an additional challenge across institutions. Tuber-like pathology may be, in fact, more diffusely present below the conventional MRI resolution, with the visually discrete tubers just representing the ‘tip of the iceberg’. The authors will discuss that large parts of normal-appearing white matter (NAWM), in fact, have an abnormal microstructure. In addition, there are other types of structural CNS abnormalities in TSC, as outlined below, which may need to be taken into account.

A second limitation of conventional MRI is the inability to identify epileptogenic tubers or perituber regions, a critical step in the presurgical evaluation of candidates for epilepsy surgery [18,19]. A third limitation is that microstructural CNS tissue characteristics of TSC, including abnormal differentiation, migration, organization, myelination and connectivity cannot be examined by conventional MRI [3,20–25].

Newer MRI techniques are used to investigate imaging correlates of neurobehavioral phenotype, epilepsy and microstructural CNS tissue properties in TSC. Diffusion-weighted MRI (DWI) probes natural barriers to the diffusion of water molecules in tissues, thereby providing information on their microstructural properties. To quantify this diffusion, multiple DWI images are used to generate a mathematical model of the diffusion. The most common model is called diffusion tensor imaging (DTI), which describes the 3D diffusion and strength with a tensor at each voxel. DTI models are consistent with known neuroanatomy and can demonstrate pathological microstructural changes of tissue in several neurological conditions, including multiple sclerosis [26], Alzheimer's disease [27] and epilepsy [28]. Using DTI, novel insights into the pathophysiology of TSC and the imaging determinants of clinical phenotype may lead to the identification of early prognostic indicators, and guide the development of targeted interventions.

The authors review the literature on DTI and tuberous sclerosis, focusing on clinical implications, as well as its contribution to the understanding of the neuropathological processes in TSC. The imaging principles of DTI and several related techniques are introduced, and future directions are discussed.

## **Structural CNS abnormalities in TSC, conventional MRI**

The intracranial lesions of TSC appear to result from abnormal expression of the genes within the germinal matrix stem cells, affecting differentiation and migration, resulting in dysplastic cells in the subependymal region, the cortex and along the cell migration pathways [29]. There are four common CNS lesions detected by conventional MRI, as described below.

### **Cortical tubers**

Cortical tubers represent focal hamartomatous regions of disorganized cortical lamination. Histopathologic examination of tubers typically reveals prominent numbers of glia, neuronal appearing cells, and giant cells that express markers of both neuronal and glial lineages [3]. They are found in the brains of at least 80% of children with TSC [30]. On MRI, they are highly characteristic moderately well-circumscribed areas of increased signal intensity on T2-weighted (T2W) images and decreased signal intensity on T1-weighted (T1W) images. The overlying cortex may bulge and the gray-white matter differentiation is reduced. They are best appreciated on fluid attenuation inversion recovery images (Figure 1A & B) [31,32]. Based on conventional imaging, tubers can be classified following the scheme of Gallagher *et al.*, which may have clinical implications [33]. The exact role of cerebellar lesions is still an active area of investigation [34], but recently a large series of 145 patients demonstrated that the MRI appearance of tubers is different in the cerebellum. Here, lesions are wedge-shaped, hyperintense on T2 and hypo- or isointense on T1. Cerebellar tubers are more likely to enhance, and the enhancement may follow the underlying cerebellar neuroanatomy [35].

### **Subependymal nodules & subependymal giant astrocytomas**

Subependymal nodules (SENs) and subependymal giant astrocytomas (SEGAs) are found adjacent to the ventricles. SENs are small and can be found anywhere along the lining of the

ventricles. SEGAs can cause obstructive hydrocephalus as they are larger than SENs and occur most commonly at the caudothalamic groove, near the foramen of Monro. They are noninvasive and non-metastatic, and also histologically benign. However, SEGAs probably arise from SENs and the distinction is primarily made on the basis of size and location typically near the foramen of Monro [3]. As not all large lesions are astrocytomas, they are sometimes referred to as subependymal giant cell tumors. Other than glial-cell elements, they also contain dysplastic giant cells that express neuronal markers, similar to tubers [3,5]. On MRI, SENs and SEGAs are iso- to hyper-intense on T1W images and variably hypointense on T2W images depending upon the extent of calcification. T2W images are optimal for showing susceptibility artifacts from calcification. Morphologically, they appear as discrete or roughly confluent areas of rounded hypertrophic tissue, bulging into the ventricle. Both can show contrast enhancement. The SENs over 5 mm in diameter which are incompletely calcified and enhanced after gadolinium administration may be at higher risk of growing into a SEGA (Figure 1C & D) [36,37].

### **White matter abnormalities**

White matter abnormalities include radial migration lines (RMLs) that appear as linear abnormalities extending from the ventricular surface to the cortical tuber. Within the high signal of the RMLs, there are linear streaks of abnormalities that are isointense to cortex, best appreciated on T2W images and nonenhanced T1W images. These represent gliosis and heterotopic glia and neurons along the course of abnormal cortical migration in the subcortical white matter. They are not always seen in relation to a tuber (Figure 1E) [36,38].

### **Discrete rounded cyst-like abnormalities**

Discrete rounded cyst-like abnormalities are found subcortically or within the deep hemispheric white matter. They have cystic properties with signal intensities comparable to cerebrospinal fluid (CSF). Recently, a strong association of these lesions was found with *TSC2* and a more severe seizure phenotype [39]. Originally thought to be static lesions derived from tuber degeneration or heterotopic tissue [38,40], their evolution over time has been clearly documented (Figure 1F) [41].

Microscopic abnormalities, such as microdysgenesis, heterotopic gray matter and lamination defects, are generally not visible at conventional MRI resolution. Rare associations with cortical malformations, such as hemimegalencephaly [42,43] and schizencephaly [44], are beyond the scope of this article. Finally, global cerebellar atrophy is reported in 4–17% of TSC patients and recently an association was shown with the presence of cerebellar tubers. Whether this is a destructive process (seizures, anti-epileptic medications, among others) or a primary developmental phenomenon is unknown [35,45].

## **DWI, DTI & tractography**

### **Diffusion-weighted imaging**

DWI allows characterization and quantitative measurement of the diffusion of water molecules in tissues. It enables distinction between unrestricted and restricted diffusion of protons, based on the random (also known as Brownian) motion of water molecules in tissue [26,46]. The most well-known indication for DWI is detection of restricted diffusion in acute ischemic stroke.

In pure water, there is no barrier to the diffusion of water molecules and the diffusion is referred to as isotropic. By contrast, in the brain, local restriction of water diffusion such as that caused by the presence of densely organized white matter fascicles, gives rise to anisotropic diffusion. The degree of anisotropy is a measure of directional preference of

diffusion and depends on the structure present in the voxel (3D pixel). In highly organized structures (e.g., white matter tracts), diffusion will be highly anisotropic, as molecules will diffuse preferably along the path of least resistance (e.g., along the axon within the myelin sheath) [26,46–48]. In less coherent structures (e.g., in a tuber consisting of poorly organized collection of cells), the diffusion will be almost isotropic.

In an MRI scanner, protons' spins are initially aligned with the strong magnetic field produced by the magnet. Applying a short magnetic pulse changes this orientation and protons' spins start to precess (much like a spinning humming top deviates from its central axis). This precession generates an electromagnetic signal detectable by an electric coil [46]. The rate of precession depends on the strength of the magnetic field. Applying a magnetic field that varies along a certain direction (adding a so-called field gradient pulse to the magnetic field), we can label the spins by different precession rates according to their position along the gradient direction. This variation in precession rates results in an interference between the precessing spins, leading to a signal loss. Applying the opposite field gradient pulse would refocus the spins and recover the signal loss, only if the protons did not move between the two pulses. However, due to motion, protons' spins are imperfectly refocused and the signal loss cannot be compensated for. The amount of remaining signal loss is related to the amount of motion that occurs in the gradient direction. Measuring the signal loss therefore measures the diffusion of protons (or water molecules that contain them). This is the physical basis of DWI.

Each DWI provides information about the diffusion along one particular direction (the gradient direction). Several DWI are thus needed to characterize the diffusion in all directions. Much like one only needs two points to characterize a linear relationship between two variables, one only needs a few DWI to estimate a diffusion model that characterizes the diffusion in all directions.

### Diffusion tensor imaging

DTI is the most widely used model of the diffusion signal in tissues. DTI models the average diffusion direction and strength at each voxel with a tensor, which can be thought of as an ellipsoid (Figure 2). This ellipsoid is characterized by a principal direction along which diffusion is the strongest. In the two orthogonal directions, diffusion is more constrained and its magnitude is given by the width of the ellipsoid in those directions. A total of six parameters are required to fully define the ellipsoid: three parameters for the widths and length (these are also called diffusivities or eigenvalues), two parameters to define the direction of strongest diffusivity and one parameter to define the rotation of the ellipsoid around its principal axis. Mathematically, ellipsoids are represented as symmetric positive-definite matrices with three rows and three columns. Diffusivities can be obtained from those matrices through a mathematical method called eigen decomposition (hence their name 'eigenvalues').

Since six parameters define the diffusion tensor (the ellipsoid), six DWI acquired for different gradient directions would in theory be enough to estimate the values of the tensor parameters. However, owing to measurement errors, a larger number of DWI is usually acquired (typically 30 directions). It is suggested to acquire as many images as time allows, and to strictly standardize acquisition details for research purposes.

The shape of the tensor provides information on the nature of the diffusion occurring in the corresponding voxel (Figure 2). Isotropic diffusion (which occurs in free water) gives rise to a spherical tensor, and its diffusivities are equal in all directions. Highly anisotropic diffusion gives rise to long and thin ellipsoids, indicating that the diffusion is highly favored along a principal direction and highly constrained in the other directions.

## DTI-based measures

DTI-based measures quantify the shape of the ellipsoids and can be used as biomarkers for diseases. Two main measures are commonly used: the mean diffusivity (MD) and the fractional anisotropy (FA). The (bulk) MD is the average diffusion in all three directions. It was measured before the introduction of the diffusion tensor model by averaging the diffusion coefficient estimated in three orthogonal directions. In practice, this apparent diffusion coefficient is used interchangeably with MD. The MD is an intrinsic property of tissues. For example, the MD of demyelinated white matter is increased as there is more extracellular water and a weaker biological barrier to diffusion [26]. The FA reflects the degree of asymmetry of the diffusion in a particular location. If the diffusion is completely isotropic (Figure 2B), then FA is equal to zero. Conversely, if the diffusion is extremely anisotropic (water molecules can only diffuse in one direction and diffusivities are zero in the other two directions), then FA is equal to one. Diffusion within the white matter axons is restricted to the longitudinal axis by cell membranes and by the myelin sheath which forms a biological barrier, resulting in a high FA. When neurons or myelin sheaths are damaged, the FA decreases; there is less preferential directionality of diffusion because the fluid can move freely along various axes [49]. MD and FA are nonspecific and can be altered by any pathological process that modifies tissue integrity and leads to a loss of structural barriers to water motion (Figure 3).

## DTI tractography

DTI tractography is a technique based on relatively recently developed postprocessing algorithms for DTI, and allows for the study of the 3D configuration of major white matter tracts [50,51]. Orientation-based color-coding (also known as color maps) is a visualization approach in which the brightness of the image represents the magnitude of preferential diffusion (i.e., FA), and red (left–right axis), green (anterior–posterior axis) and blue (inferior–superior axis) indicate fascicle orientation. This color scheme assumes that the preferential diffusion axis coincides with the orientation of the fascicle, as explained above (Figure 4) [52]. To generate tracts, the main direction of the tensors (longest arrow in Figure 2) is followed from one voxel to another.

Based on the contiguity of adjacent voxels with a highly similar preferential diffusion axis, 3D tracts can be generated that represent the course of a major white matter pathway. The tract is formed by stepping along the line in both ortho- and retro-grade directions according to the fascicle orientation (imagine a tract formed by a series of lined-up cucumbers) [26]. The tract starts at a seeding point, which is often defined manually by the examiner who delineates a certain region of interest. Regions of interest can be determined by (semi)automated techniques (e.g., functional MRI, or segmentation algorithms that isolate structures on conventional MRI).

## Specifics of reconstructed tracts

The specifics of the reconstructed tracts are dependent on important modifiers that terminate the tract-generating algorithm when boundary conditions are met. Examples include the maximum angle a tract is allowed to make, the cutoff value of FA below which the next voxel is no longer considered to be part of the tract (stopping when the tensor is spherical and has an insufficient degree of anisotropy) and the FA-momentum, which permits the tract-generating algorithm to go through an aberrant voxel with a poor FA if the previous few voxels in the tract had a high FA value, for instance carry momentum. This last modifier allows the tract generation not to stop prematurely. In both clinical and research applications of tractography, the exact parameters should always be scrutinized closely. Notably, the 3D tracts are not a (micro-)structural reality, but are traces of the major pathways representing white matter fascicles by means of connected diffusion tensors. The DTI tractography



method has been validated with post-mortem anatomic and animal studies, showing good agreement [52,53].

### **Microstructural tissue**

Microstructural tissue properties are reflected by FA and MD values of anatomical structures such as major white matter pathways (e.g., corpus callosum and language pathways) or specific regions of interest (e.g., neoplasm or tuber). A well-established relation between DTI parameters and tissue properties is not limited to only animal models, but is also present in humans. Changes in axonal integrity and diameter can affect axial diffusivity (the mean diffusion along the axial axis) [54]. Radial diffusivity (mean diffusion orthogonal to the longitudinal axis) values correlate with myelination in the normally developing mouse brain and in experimental dysmyelination [53,55,56]. FA relates to axonal packing, organization and myelination [57,58]. With tractography or with segmentation, an anatomically relevant collection of voxels can be selected for analysis. The investigation of local microstructural information in a noninvasive manner is unique and has propelled the widespread use of DWI and DTI in the clinical and research setting over the past decade.

### **Limitations of the DTI model**

#### **Heterogeneous fascicle orientations**

The DTI model assumes that at each voxel, the diffusion is Gaussian with at most one preferential direction. This assumption is reasonable only when all axons in the voxel are aligned in a specific orientation. However, owing to the presence of complex fascicle organization, heterogeneous fascicle orientations can be present in one voxel [59,60]. In the corona radiata, for example, corticospinal tracts cross fascicles of the corpus callosum (Figure 5). Another example are the pyramidal projections that give rise to fanning fascicles (i.e., fascicles that follow different directions from an original point at which they are aligned) [61]. Recent studies estimate the prevalence of those heterogeneities to range between 60 and 90% of voxels in the white matter [62]. When fascicles are crossing, kissing or fanning, interpretation of the DTI-based measures (MD and FA) may be misleading [63]. For instance, in the presence of two crossing fascicles, a single overly wide tensor would be estimated resulting in a decreased FA (Figure 5). This decreased FA is not related to a property of the fascicle and if interpreted this way may lead to the wrong assumption that the myelin integrity is altered for that fascicle.

#### **Partial voluming effects**

Voxels that are at the interface between different tissues (gray and white matter), between adjacent fiber bundles or between a tissue and CSF suffer another problem called partial voluming. The diffusion signal arising from protons in the different compartments (CSF, gray or white matter) will be averaged into a single value that is observed in DWI. Because DTI assumes that a single fascicle is present in the voxel, influences of different compartments will conflate, resulting in an inflated tensor with a lower FA. As with heterogeneous fascicle orientations, this decreased FA may be misleadingly interpreted as altered myelin.

Novel diffusion modeling methods that attempt to address these problems will be discussed in the future perspective section.

## Structural CNS abnormalities & DTI

### Cortical tubers

The first report on DWI and TSC stems from 2001 [64]. Tubers appear as structures with a decreased FA and increased MD, corresponding to tissue findings of poorly organized collections of dysplastic and large cells [3]. Although fluid attenuation inversion recovery imaging provides high-contrast images that allow for delineation of tubers, DTI imaging often reveals a larger area of perituberal diffusion abnormalities. This increased diffusivity may better reflect the true extent of tuber pathology, at times demonstrating contiguity of tissue abnormalities between adjacent tubers, and a more gradual change to NAWM [65–67]. As tubers are prominent abnormalities, extensive research has been carried out on the relationship between tuber burden, location and clinical phenotype. Tuber burden has been quantified through counting numbers [10], calculation of total volume [68] or of relative volume as compared with white matter or total brain volume [16]. Although a relation has been established between tuber burden and the extent of white matter DTI abnormalities [68], the extent of SENs and RMLs also correlate with measures of tuber pathology, which is not surprising as histopathologically these lesions have common features too [69]. These relations suggest that widespread migration and differentiation abnormalities are present and the burden of any of these abnormalities is likely to be reflected in the broad neurophenotypical outcome.

### SENs & SEGAs

There are no studies of the DTI properties of SENs and SEGAs available. Currently, a SEN that exceeds 1 cm in diameter, enhances with gadolinium contrast enhancement, and is not calcified is considered at high-risk for developing into a SEGA, although there is both a pathologic and a radiologic continuum between the two [70]. Early differentiation of SEGAs from SENs before the foramen of Monro is obstructed may provide opportunity to prevent hydrocephalus and associated morbidity and mortality [71,72]. SEGAs can grow fast, and once repeat imaging shows interval growth, resolution or stabilization have not been reported [73]. With serial DTI, it would be of interest to examine whether any microstructural differences between SENs and SEGAs could be established, and if such findings carry prognostic value.

### White matter abnormalities & NAWM

A growing body of work, summarized in [23], has used DTI to describe abnormalities in white matter that appears normal on conventional imaging, referred to as NAWM [23–25,67,68,74,75]. DTI abnormalities are not limited to perituberal white matter [66,76,77], as myelination, migration and differentiation abnormalities extend beyond the discrete boundary of tubers described by conventional T2W (fluid attenuation inversion recovery) imaging. This has important implications as it is in concordance with findings of a global or diffuse microstructural white matter pathology found in neuropathological studies of TSC [78], in addition to multifocal tuber pathology [79]. Many regions have been implicated in DTI studies of the NAWM, but heterogeneity in the study population, image acquisition and processing, and statistical approach make synthesis of this work challenging. The presence of DTI abnormalities may be ubiquitous throughout the white matter [23].

In TSC, animal models provide a potential explanation for the abnormal diffusion characteristics. The diameter and integrity of the axon can affect axial diffusivity and the amount of diffusion according to the longitudinal axis. In the authors' laboratory, the *Tsc1c/cSynI-Cre<sup>+</sup>* mouse model has an increased axonal diameter [Sahin M *et al.*, Unpublished Data]. Radial diffusivity, the amount of diffusion perpendicular to the longitudinal axis, is dependent on myelination and the presence of extracellular changes such as glial and giant



cells. In TSC, increased radial diffusivity may indicate poor myelination (thickness, integrity or permeability) or increased presence of extracellular material, impairing the biological barrier to diffusion in the radial direction. Indeed, hypomyelination [21] and aberrant neuronal organization [22] have been shown in animal models of TSC. A decreased FA may represent abnormal organization, packing or myelination of axons. In mouse models of TSC, loss of *Tsc1* or *Tsc2* is associated with abnormal neuronal connectivity – specifically neuronal polarity, axon formation and guidance [20–22].

Recently, the view of diffuse microstructural abnormality in the white matter was challenged. van Eeghen *et al.* found no differences in the NAWM of TSC patients compared with controls, once migrational abnormalities visible on conventional imaging were excluded from the analysis of white matter, and the RMLs accounted for the DTI abnormalities of the NAWM. This work should be reproduced as it would imply TSC is characterized by multifocal but not ubiquitous abnormalities in white matter connectivity [69]. Even with the view of TSC as a multifocal migrational disorder, DTI is supported as a putative biomarker for neurocognitive morbidity in TSC.

Finally, small animal imaging studies of TSC rodent models or imaging data of human pathological specimen are much needed to better establish the relation between DTI abnormalities and TSC pathology.

## Epilepsy, epilepsy surgery & DTI

### Epilepsy

Epilepsy, in particular, infantile spasms and early-onset refractory seizures have predictive value for poor cognitive outcome [16,80,81]. Early control may be associated with improved outcome [82,83]. However, this relation is inconsistent on an individual patient level. Moreover, heterozygous mouse models of TSC have failed to replicate typical neuroanatomical findings of human patients with TSC (SEGAs, tubers and SENs), and have neither neuropathological abnormalities nor seizures, yet demonstrate cognitive and behavioral abnormalities [34]. In these same animal models the presence of epilepsy is again detrimental, worsening the neurophenotype. In short, early and complete seizure control is critical for neurodevelopmental outcome.

Abnormal diffusion can result from recurrent seizures and status epilepticus through various mechanisms including excitocytotoxic edema and neuronal cell-death, axonal damage and subsequent wallerian degeneration, systemic effects including vasoconstriction and hypoxia, antiepileptic drugs, secondary maladaptive developmental changes and plasticity-related reorganization of local and widespread connections [84]. In TSC, tubers have a relatively decreased FA and increased MD, and more so in epileptogenic compared with silent tubers [19,85]. The pathophysiology of these DTI changes is unclear; it could be a poorer microstructural integrity responsible for more severe epileptic properties, or conversely, local changes as a result from more epileptic discharges or both.

How varying levels of structural integrity of tubers relates to clinical manifestations of epilepsy is still subject to ongoing study. In 2010, a relationship was found between increased epilepsy severity and the predominance of poorly organized tubers on conventional imaging [33]. Apparent diffusion coefficient measures of the dominant tuber type confirmed quantitative differences in the subgroups. From the same researchers, again mainly based on conventional imaging, an association between cyst-like tubers (with by definition an exceptional low tissue integrity) and an aggressive seizure phenotype of infantile spasms and medically refractory seizures has been reported [39,41,86]. Thus, the evolution of DTI characteristics of (peri-)tuberal microstructure over time, and the

relationship to epileptogenicity and epilepsy severity, are currently being studied in our laboratory.

### **Epilepsy surgery**

Seizures arise in the vicinity of tubers, yet the specific origin of epileptiform activity is debated. Two studies have found seizures to originate from the tuber tissue itself [87,88] while others have indicated the perituberal tissue to be the source of epileptiform activity [89,90]. By contrast, many tubers are not epileptogenic at all, and anecdotally some patients have epilepsy in the absence of tubers on structural imaging.

For medically refractory seizures, resective epilepsy surgery typically consists of a tubectomy. Clinical examination, seizure semiology, multiple imaging and neurophysiologic modalities are combined to identify epileptogenic tubers [87,91]. A recent report also suggests the potential use of magnetic resonance spectroscopy [92], a review of which is outside the scope of this paper. Using DTI, two studies with a total of 19 patients have independently reported a lower FA and higher MD in epileptogenic compared with nonepileptogenic tubers [19,85]. The main focus of epileptic activity remains stable in most patients [93]. With the routine availability of DTI as opposed to additional patient burden, high cost and required expertise for other advanced auxiliary studies in the workup for epilepsy surgery, it is imperative that the predictive value of DTI in epileptogenic tuber identification in TSC be studied on a larger scale (Figure 6).

## **Autism, cognition & DTI**

### **Intellectual disability**

Three lines of imaging research are explored as potential explanations for neurocognitive deficits in TSC. First, as outlined in the introduction, the number, location (frontal or occipital) and total volume of tubers have been associated with intellectual disability [15,16,94]. However, in clinical practice patients without tubers may have disabling symptoms while others with large tuber burden can have few neurologic symptoms. In 25 high-functioning adults with TSC and a normal intelligence, tuber burden was not correlated with cognitive measures [95]. Non tuber pathologies, including the frequency of SENs and RMLs, also appear to correlate with neurological phenotype [69].

Second, the cerebellum has been implicated, given its smaller size, in a morphometric study [45], which revealed the presence of lesions in more than a quarter of patients [11]. An association of ASD with PET abnormalities of the cerebellar white matter and of deep cerebellar nuclei has been made [96,97]. Recently, our group showed that loss of *Tsc1* in mouse cerebellar Purkinje cells results in autistic-like behaviors [98].

Third, in various studies DTI has revealed widespread abnormalities in the NAWM, suggesting a role for aberrant microstructural connectivity in the pathophysiological mechanism of neurocognitive deficits. Typically study populations have not been sufficiently large to study detailed neuropsychological outcome data, other than presence of a diagnosis of autism [23,24]. A large, prospective, multicenter trial is underway to study neurocognitive effects of mTOR inhibitors (mTOR-is) but unfortunately, these subjects will not undergo imaging as part of this study.

### **Autism**

In humans, TSC and decreased microstructural integrity of the corpus callosum and of the language pathways have been associated with ASD in two large DTI studies (Figure 7) [23,24]. While these were the first studies to correlate DTI with outcome, they were limited

by the retrospective design, the binary nature of the diagnosis of autism and the potential confounders of intelligence measures and epilepsy severity. A prospective study is important because while classically ASD can be associated with normal or even superior intelligence, it appears in TSC that ASD and intellectual disabilities may co-occur [99]. On the other hand, there is a growing body of literature on idiopathic ASD and DTI abnormalities in the NAWM, including but not limited to the corpus callosum [100,101] and the arcuate fasciculus [102], reviewed elsewhere [103]. Aberrant long-range connectivity is central to the theory of autism as a developmental disconnection disorder, in which there is decreased integration of cognitive information from functionally separate and distant brain regions into a coherent, higher order concept [104]. In summary, abnormal microstructural connectivity is found in DTI studies of ASD, both with and without a concurrent diagnosis of TSC, which validates TSC as a natural model to study the development of autism. Indeed, in a recent electroencephalogram-based cross-disorder study of patients with TSC alone, TSC with ASD, and ASD without TSC, abnormal functional connectivity was associated with ASD regardless of the etiology [105]. An NIH-funded multicenter Autism Center of Excellence study has just been launched to prospectively study imaging and EEG predictors of neurophenotypical outcome, including autism, intellectual deficit and epilepsy.

## Conclusion

TSC is a genetic, neurocutaneous, multiorgan disorder with potentially devastating sequelae including intractable epilepsy, intellectual impairment and ASD. There is a poor genotype–phenotype correlation and to date no conventional imaging biomarker reliably relates to neurophenotype. DTI is able to quantify microstructural tissue water diffusion properties, and reflects underlying pathology in TSC. With significant advances in the understanding of the molecular biology, the reversal of neurological comorbidity in mouse models, the clinical trials of mTOR-is for epilepsy and cognition, the potential of DTI as a biologically meaningful biomarker in TSC becomes even more important.

## Future perspective

Novel diffusion models allow for more biologically accurate qualification of microstructural properties. Over the next few years, these models will yield additional insights in human TSC in a noninvasive manner. Moreover, with the emergent use of mTOR-is, it will be important to establish a good biomarker that reliably corresponds to epilepsy and cognitive and behavioral outcome measures. DTI may prove to meet these requirements, and facilitate larger interventional trials.

## Novel diffusion models

To overcome the aforementioned limitations of DTI, novel diffusion models have been proposed. One natural generalization of DTI is the development of multitensor models (also called multi-fiber and -fascicle models) [106]. Instead of assuming that a single fascicle is present in the voxel, multitensor models represent each fascicle present in the voxel with its own tensor (Figure 5D). With such a model, DTI-based measures (FA and MD) can be evaluated for each fascicle independently [107]. This solves the problem of artificially lower FA in areas with heterogeneous fascicle orientations. Furthermore, tissues with isotropic diffusion and CSF can be represented by an isotropic tensor (a sphere) and be included as one of the tensors in the multitensor model, thereby solving the partial voluming problem.

As these models are being defined by more parameters, they also require more DWI. However, recent developments have shown that we can estimate a multitensor model from 45 DWI [108] or even 30 DWI [109]. Imaging time with those novel techniques does not exceed 10 min and is therefore achievable in the clinical setting. Multitensor models also

require novel methods to estimate them. In particular, one challenge is to estimate how many fascicles are present in the voxel. Recent methods have been developed to solve this problem in an automatic fashion [110].

Besides overcoming the limitations of DTI, novel diffusion models open new opportunities to investigate the white matter microstructure. For instance, the amount of isotropic diffusion in the white matter has been related to the presence of neuroinflammation or edema [111]. Comprehensive studies of the white matter microstructure allow us to distinguish between axon and myelin injury, cell infiltration and axonal loss [112].

### The mTOR pathway, mTOR-is & DTI as a putative biomarker

*TSC1* and *TSC2* genes encode for hamartin and tuberlin, respectively. These bind to form a protein complex that modulates the mTOR kinase, which plays a key role in the regulation of protein synthesis [113]. In the absence of a functional TSC protein complex, mTOR is overactive with subsequent disinhibited protein synthesis and cell growth [114]. Besides cell growth, mouse models have shown the TSC proteins play a critical role in axonal, dendritic and synaptic development and function, briefly reviewed here [115]. Loss of *Tsc1* or *Tsc2* function results in aberrant connectivity on a cellular level, and in mouse models is associated with seizures and neurobehavioral abnormalities. mTOR-i have a mechanism of action that virtually directly addresses the molecular defect in TSC, are safe and effective for treatment of SEGAs [73,116], and may also be safe in children under 3 years of age [117]. With DTI, microstructural changes of the white matter have been reported with the use of mTOR-i in patients with SEGA [79].

### Epilepsy

In TSC mouse models, mTOR-i can prevent, improve and even stop seizures [118–120]. Accumulating evidence from small case-series and from larger SEGA treatment trials show that mTOR-is have anti-epileptic and potentially even anti-epileptogenic properties [120]. However, the neuroanatomic phenotype responds only partly, or not at all, to such intervention. A large multicenter trial is currently underway for everolimus (Afinitor<sup>®</sup>, Novartis, Inc., NJ, USA) as adjunct therapy for refractory partial complex seizures in TSC. DTI changes related to altered seizure control will be examined in a subset of the study population.

### Cognition & autism

The defects in axonal, dendritic and synaptic development in TSC may well be related to neurobehavioral, cognitive and autistic symptoms in these patients. In mouse models, mTOR-i improve learning and prevent autistic features [98,121]. Given the first report of improvement of white matter microstructure with mTOR-is in humans [79], and the relation between autism and white matter microstructure [23], it will be exciting to investigate whether changes in DTI properties parallel the cognitive and neurobehavioral changes in patients currently studied in the Autism Centers of Excellence network, and in subgroup analysis of the SEGA Phase III treatment trial. If so, DTI will become a biomarker for cognition in TSC, facilitating future therapeutic developments over the next few years, and allowing for exploration of mTOR-is in several genetic causes of autism.

### References

Papers of special note have been highlighted as:

- of interest

■ ■ of considerable interest

1. Crino PB, Nathanson KL, Henske EP. The tuberous sclerosis complex. *N Engl J Med*. 2006; 355(13):1345–1356. [PubMed: 17005952]
2. Osborne JP, Fryer A, Webb D. Epidemiology of tuberous sclerosis. *Ann NY Acad Sci*. 1991; 615:125–127. [PubMed: 2039137]
3. Ess KC. The neurobiology of tuberous sclerosis complex. *Semin Pediatr Neurol*. 2006; 13(1):37–42. [PubMed: 16818174]
4. Jentarra G, Snyder SL, Narayanan V. Genetic aspects of neurocutaneous disorders. *Semin Pediatr Neurol*. 2006; 13(1):43–47. [PubMed: 16818175]
5. Curatolo P, Bombardieri R, Jozwiak S. Tuberous sclerosis. *Lancet*. 2008; 372(9639):657–668. [PubMed: 18722871]
6. Roach ES, Gomez MR, Northrup H. Tuberous sclerosis complex consensus conference: revised clinical diagnostic criteria. *J Child Neurol*. 1998; 13(12):624–628. [PubMed: 9881533]
7. Datta AN, Hahn CD, Sahin M. Clinical presentation and diagnosis of tuberous sclerosis complex in infancy. *J Child Neurol*. 2008; 23(3):268–273. [PubMed: 18230839]
8. Dabora SL, Jozwiak S, Franz DN, et al. Mutational analysis in a cohort of 224 tuberous sclerosis patients indicates increased severity of *TSC2*, compared with *TSC1*, disease in multiple organs. *Am J Hum Genet*. 2001; 68(1):64–80. [PubMed: 11112665]
9. Jeste SS, Sahin M, Bolton P, Ploubidis GB, Humphrey A. Characterization of autism in young children with tuberous sclerosis complex. *J Child Neurol*. 2008; 23(5):520–525. [PubMed: 18160549]
10. Bolton PF, Park RJ, Higgins JN, Griffiths PD, Pickles A. Neuro-epileptic determinants of autism spectrum disorders in tuberous sclerosis complex. *Brain*. 2002; 125(Pt 6):1247–1255. [PubMed: 12023313]
11. Eluvathingal TJ, Behen ME, Chugani HT, et al. Cerebellar lesions in tuberous sclerosis complex: neurobehavioral and neuroimaging correlates. *J Child Neurol*. 2006; 21(10):846–851. [PubMed: 17005099]
12. Walz NC, Byars AW, Egelhoff JC, Franz DN. Supratentorial tuber location and autism in tuberous sclerosis complex. *J Child Neurol*. 2002; 17(11):830–832. [PubMed: 12585723]
13. Weber AM, Egelhoff JC, McKellop JM, Franz DN. Autism and the cerebellum: evidence from tuberous sclerosis. *J Autism Dev Disord*. 2000; 30(6):511–517. [PubMed: 11261463]
14. Wong V. Study of the relationship between tuberous sclerosis complex and autistic disorder. *J Child Neurol*. 2006; 21(3):199–204. [PubMed: 16901420]
15. Goodman M, Lamm SH, Engel A, Shepherd CW, Houser OW, Gomez MR. Cortical tuber count: a biomarker indicating neurologic severity of tuberous sclerosis complex. *J Child Neurol*. 1997; 12(2):85–90. [PubMed: 9075016]
16. Jansen FE, Vincken KL, Algra A, et al. Cognitive impairment in tuberous sclerosis complex is a multifactorial condition. *Neurology*. 2008; 70(12):916–923. Studies the relationship between clinical (epilepsy), imaging and neuropsychological variables. [PubMed: 18032744]
17. Wong V, Khong PL. Tuberous sclerosis complex: correlation of magnetic resonance imaging (MRI) findings with comorbidities. *J Child Neurol*. 2006; 21(2):99–105. [PubMed: 16566871]
18. Asano E, Chugani DC, Muzik O, et al. Multimodality imaging for improved detection of epileptogenic foci in tuberous sclerosis complex. *Neurology*. 2000; 54(10):1976–1984. [PubMed: 10822440]
19. Jansen FE, Braun KP, van Nieuwenhuizen O, et al. Diffusion-weighted magnetic resonance imaging and identification of the epileptogenic tuber in patients with tuberous sclerosis. *Arch Neurol*. 2003; 60(11):1580–1584. [PubMed: 14623730]
20. Choi YJ, Di Nardo A, Kramvis I, et al. Tuberous sclerosis complex proteins control axon formation. *Genes Dev*. 2008; 22(18):2485–2495. [PubMed: 18794346]
21. Meikle L, Talos DM, Onda H, et al. A mouse model of tuberous sclerosis: neuronal loss of *Tsc1* causes dysplastic and ectopic neurons, reduced myelination, seizure activity, and limited survival. *J Neurosci*. 2007; 27(21):5546–5558. [PubMed: 17522300]

22. Nie D, Di Nardo A, Han JM, et al. Tsc2–Rheb signaling regulates EphA-mediated axon guidance. *Nat Neurosci.* 2010; 13(2):163–172. [PubMed: 20062052]
23. Peters JM, Sahin M, Vogel-Farley VK, et al. Loss of white matter microstructural integrity is associated with adverse neurological outcome in tuberous sclerosis complex. *Acad Radiol.* 2012; 19(1):17–25. First report of sufficient power to suggest a relationship between diffusion tensor imaging of the white matter and neurocognitive phenotype in tuberous sclerosis complex. [PubMed: 22142677]
24. Lewis WW, Sahin M, Scherrer B, et al. Impaired language pathways in tuberous sclerosis complex patients with autism spectrum disorders. *Cereb Cortex.* 2013; 23(7):1526–1532. [PubMed: 22661408]
25. Krishnan ML, Commowick O, Jeste SS, et al. Diffusion features of white matter in tuberous sclerosis with tractography. *Pediatr Neurol.* 2010; 42(2):101–106. [PubMed: 20117745]
26. Goldberg-Zimring D, Mewes AU, Maddah M, Warfield SK. Diffusion tensor magnetic resonance imaging in multiple sclerosis. *J Neuroimaging.* 2005; 15(Suppl 4):S68–S81.
27. Bozzali M, Falini A, Franceschi M, et al. White matter damage in Alzheimer's disease assessed in vivo using diffusion tensor magnetic resonance imaging. *J Neurol Neurosurg Psychiatry.* 2002; 72(6):742–746. [PubMed: 12023417]
28. Luat AF, Chugani HT. Molecular and diffusion tensor imaging of epileptic networks. *Epilepsia.* 2008; 49(Suppl 3):15–22. [PubMed: 18304252]
29. Curatolo P, Verdecchia M, Bombardieri R. Tuberous sclerosis complex: a review of neurological aspects. *Eur J Paediatr Neurol.* 2002; 6(1):15–23. [PubMed: 11993952]
30. Crino PB, Henske EP. New developments in the neurobiology of the tuberous sclerosis complex. *Neurology.* 1999; 53(7):1384–1390. [PubMed: 10534239]
31. Kato T, Yamanouchi H, Sugai K, Takashima S. Improved detection of cortical and subcortical tubers in tuberous sclerosis by fluid-attenuated inversion recovery MRI. *Neuroradiology.* 1997; 39(5):378–380. [PubMed: 9189887]
32. Takanashi J, Sugita K, Fujii K, Niimi H. MR evaluation of tuberous sclerosis: increased sensitivity with fluid-attenuated inversion recovery and relation to severity of seizures and mental retardation. *AJNR Am J Neuroradiol.* 1995; 16(9):1923–1928. [PubMed: 8693996]
33. Gallagher A, Grant EP, Madan N, Jarrett DY, Lyczkowski DA, Thiele EA. MRI findings reveal three different types of tubers in patients with tuberous sclerosis complex. *J Neurol.* 2010; 257(8):1373–1381. [PubMed: 20352250]
34. Tsai P, Sahin M. Mechanisms of neurocognitive dysfunction and therapeutic considerations in tuberous sclerosis complex. *Curr Opin Neurol.* 2011; 24(2):106–113. [PubMed: 21301339]
35. Vaughn J, Hagiwara M, Katz J, et al. MRI characterization and longitudinal study of focal cerebellar lesions in a young tuberous sclerosis cohort. *AJNR Am J Neuroradiol.* 2013; 34(3):655–659. [PubMed: 22954744]
36. Kalantari BN, Salamon N. Neuroimaging of tuberous sclerosis: spectrum of pathologic findings and frontiers in imaging. *AJR Am J Roentgenol.* 2008; 190(5):W304–309. [PubMed: 18430816]
37. Nababout R, Santos M, Rolland Y, Delalande O, Dulac O, Chiron C. Early diagnosis of subependymal giant cell astrocytoma in children with tuberous sclerosis. *J Neurol Neurosurg Psychiatry.* 1999; 66(3):370–375. [PubMed: 10084537]
38. Griffiths PD, Bolton P, Verity C. White matter abnormalities in tuberous sclerosis complex. *Acta Radiol.* 1998; 39(5):482–486. [PubMed: 9755694]
39. Chu-Shore CJ, Major P, Montenegro M, Thiele E. Cyst-like tubers are associated with TSC2 and epilepsy in tuberous sclerosis complex. *Neurology.* 2009; 72(13):1165–1169. [PubMed: 19332694]
40. Rott HD, Lemcke B, Zenker M, Huk W, Horst J, Mayer K. Cyst-like cerebral lesions in tuberous sclerosis. *Am J Med Genet.* 2002; 111(4):435–439. [PubMed: 12210306]
41. Chu-Shore CJ, Frosch MP, Grant PE, Thiele EA. Progressive multifocal cystlike cortical tubers in tuberous sclerosis complex: clinical and neuropathologic findings. *Epilepsia.* 2009; 50(12):2648–2651. [PubMed: 19624715]
42. Galluzzi P, Cerase A, Strambi M, Buoni S, Fois A, Venturi C. Hemimegalencephaly in tuberous sclerosis complex. *J Child Neurol.* 2002; 17(9):677–680. [PubMed: 12503644]



43. Griffiths PD, Gardner SA, Smith M, Rittey C, Powell T. Hemimegalencephaly and focal megalencephaly in tuberous sclerosis complex. *AJNR Am J Neuroradiol.* 1998; 19(10):1935–1938. [PubMed: 9874550]
44. Huntsman RJ, Sinclair DB, Richer LP. Tuberous sclerosis with open lipped schizencephaly. *Pediatr Neurol.* 2006; 34(3):231–234. [PubMed: 16504795]
45. Weisenfeld NI, Peters JM, Tsai PT, et al. A magnetic resonance imaging study of cerebellar volume in tuberous sclerosis complex. *Pediatr Neurol.* 2013; 48(2):105–110. [PubMed: 23337002]
46. Bitar R, Leung G, Perng R, et al. MR pulse sequences: what every radiologist wants to know but is afraid to ask. *Radiographics.* 2006; 26(2):513–537. Entry-level review regarding the physics of MRI and different acquisition schemes. [PubMed: 16549614]
47. Le Bihan D, Breton E, Lallemand D, Grenier P, Cabanis E, Laval-Jeantet M. MR imaging of intravoxel incoherent motions: application to diffusion and perfusion in neurologic disorders. *Radiology.* 1986; 161(2):401–407. [PubMed: 3763909]
48. Pierpaoli C, Jezzard P, Bassar PJ, Barnett A, Di Chiro G. Diffusion tensor MR imaging of the human brain. *Radiology.* 1996; 201(3):637–648. [PubMed: 8939209]
49. Piao C, Yu A, Li K, Wang Y, Qin W, Xue S. Cerebral diffusion tensor imaging in tuberous sclerosis. *Eur J Radiol.* 2009; 71(2):249–252. [PubMed: 18538521]
50. Bassar PJ, Pajevic S, Pierpaoli C, Duda J, Aldroubi A. *In vivo* fiber tractography using DT-MRI data. *Magn Reson Med.* 2000; 44(4):625–632. [PubMed: 11025519]
51. Mori S, Kaufmann WE, Pearlson GD, et al. *In vivo* visualization of human neural pathways by magnetic resonance imaging. *Ann Neurol.* 2000; 47(3):412–414. [PubMed: 10716271]
52. Wakana S, Jiang H, Nagae-Poetscher LM, van Zijl PC, Mori S. Fiber tract-based atlas of human white matter anatomy. *Radiology.* 2004; 230(1):77–87. [PubMed: 14645885]
53. Jiang Y, Johnson GA. Microscopic diffusion tensor imaging of the mouse brain. *Neuroimage.* 2009; 50(2):465–471. [PubMed: 20034583]
54. Budde MD, Xie M, Cross AH, Song SK. Axial diffusivity is the primary correlate of axonal injury in the experimental autoimmune encephalomyelitis spinal cord: a quantitative pixelwise analysis. *J Neurosci.* 2009; 29(9):2805–2813. [PubMed: 19261876]
55. Song SK, Yoshino J, Le TQ, et al. Demyelination increases radial diffusivity in corpus callosum of mouse brain. *Neuroimage.* 2005; 26(1):132–140. [PubMed: 15862213]
56. Sun SW, Liang HF, Trinkaus K, Cross AH, Armstrong RC, Song SK. Noninvasive detection of cuprizone induced axonal damage and demyelination in the mouse corpus callosum. *Magn Reson Med.* 2006; 55(2):302–308. [PubMed: 16408263]
57. Beaulieu C, Allen PS. Determinants of anisotropic water diffusion in nerves. *Magn Reson Med.* 1994; 31(4):394–400. [PubMed: 8208115]
58. Gulani V, Webb AG, Duncan ID, Lauterbur PC. Apparent diffusion tensor measurements in myelin-deficient rat spinal cords. *Magn Reson Med.* 2001; 45(2):191–195. [PubMed: 11180424]
59. Bandettini PA. What's new in neuroimaging methods? *Ann NY Acad Sci.* 2009; 1156:260–293. [PubMed: 19338512]
60. Mori S, van Zijl PC. Fiber tracking: principles and strategies – a technical review. *NMR Biomed.* 2002; 15(7–8):468–480. [PubMed: 12489096]
61. Tournier JD, Mori S, Leemans A. Diffusion tensor imaging and beyond. *Magn Reson Med.* 2011; 65(6):1532–1556. [PubMed: 21469191]
62. Jeurissen B, Leemans A, Tournier JD, Jones DK, Sijbers J. Investigating the prevalence of complex fiber configurations in white matter tissue with diffusion magnetic resonance imaging. *Hum Brain Mapp.* 2012 Epub ahead of print. 10.1002/hbm.22099
63. Vos SB, Jones DK, Jeurissen B, Viergever MA, Leemans A. The influence of complex white matter architecture on the mean diffusivity in diffusion tensor MRI of the human brain. *Neuroimage.* 2011; 59(3):2208–2216. [PubMed: 22005591]
64. Sener RN. Tuberous sclerosis: diffusion MRI findings in the brain. *Eur Radiol.* 2002; 12(1):138–143. [PubMed: 11868090]

65. Widjaja E, Simao G, Mahmoodabadi SZ, et al. Diffusion tensor imaging identifies changes in normal-appearing white matter within the epileptogenic zone in tuberous sclerosis complex. *Epilepsy Res.* 2010; 89(2–3):246–253. [PubMed: 20129760]
66. Garaci FG, Floris R, Bozzao A, et al. Increased brain apparent diffusion coefficient in tuberous sclerosis. *Radiology.* 2004; 232(2):461–465. [PubMed: 15215545]
67. Makki MI, Chugani DC, Janisse J, Chugani HT. Characteristics of abnormal diffusivity in normal-appearing white matter investigated with diffusion tensor MR imaging in tuberous sclerosis complex. *AJNR Am J Neuroradiol.* 2007; 28(9):1662–1667. [PubMed: 17893226]
68. Simao G, Raybaud C, Chuang S, Go C, Snead OC, Widjaja E. Diffusion tensor imaging of commissural and projection white matter in tuberous sclerosis complex and correlation with tuber load. *AJNR Am J Neuroradiol.* 2010; 31(7):1273–1277. [PubMed: 20203114]
69. van Eeghen AM, Terán LO, Johnson J, Pulsifer MB, Thiele EA, Caruso P. The neuroanatomical phenotype of tuberous sclerosis complex: focus on radial migration lines. *Neuroradiology.* 2013; 55(8):1007–1014. [PubMed: 23644537]
70. Clarke MJ, Foy AB, Wetjen N, Raffel C. Imaging characteristics and growth of subependymal giant cell astrocytomas. *Neurosurg Focus.* 2006; 20(1):E5. [PubMed: 16459995]
71. Moavero R, Pinci M, Bombardieri R, Curatolo P. The management of subependymal giant cell tumors in tuberous sclerosis: a clinician's perspective. *Childs Nerv Syst.* 2011; 27(8):1203–1210. [PubMed: 21305305]
72. Berhouma M. Management of subependymal giant cell tumors in tuberous sclerosis complex: the neurosurgeon's perspective. *World J Pediatr.* 6(2):103–110. [PubMed: 20490765]
73. Krueger DA, Care MM, Holland K, et al. Everolimus for subependymal giant-cell astrocytomas in tuberous sclerosis. *N Engl J Med.* 2010; 363(19):1801–1811. [PubMed: 21047224]
74. Peng SS, Lee WT, Wang YH, Huang KM. Cerebral diffusion tensor images in children with tuberous sclerosis: a preliminary report. *Pediatr Radiol.* 2004; 34(5):387–392. [PubMed: 15029464]
75. Arulrajah S, Ertan G, Jordan L, et al. Magnetic resonance imaging and diffusion-weighted imaging of normal-appearing white matter in children and young adults with tuberous sclerosis complex. *Neuroradiology.* 2009; 51(11):781–786. [PubMed: 19603155]
76. Karadag D, Mentzel HJ, Gullmar D, et al. Diffusion tensor imaging in children and adolescents with tuberous sclerosis. *Pediatr Radiol.* 2005; 35(10):980–983. [PubMed: 16170442]
77. Firat AK, Karakas HM, Erdem G, Yakinci C, Bicak U. Diffusion weighted MR findings of brain involvement in tuberous sclerosis. *Diagn Interv Radiol.* 2006; 12(2):57–60. [PubMed: 16752348]
78. Marcotte L, Aronica E, Baybis M, Crino PB. Cytoarchitectural alterations are widespread in cerebral cortex in tuberous sclerosis complex. *Acta Neuropathol.* 2012; 123(5):685–693. Demonstrates widespread microstructural pathology in tuberous sclerosis complex. [PubMed: 22327361]
79. Tillema JM, Leach JL, Krueger DA, Franz DN. Everolimus alters white matter diffusion in tuberous sclerosis complex. *Neurology.* 2012; 78(8):526–531. Suggests that diffusion tensor imaging parameters of white matter may improve with the use of mTOR inhibitors, indicating microstructural alterations. [PubMed: 22262746]
80. Numis AL, Major P, Montenegro MA, Muzykewicz DA, Pulsifer MB, Thiele EA. Identification of risk factors for autism spectrum disorders in tuberous sclerosis complex. *Neurology.* 2011; 76(11):981–987. [PubMed: 21403110]
81. Muzykewicz DA, Costello DJ, Halpern EF, Thiele EA. Infantile spasms in tuberous sclerosis complex: prognostic utility of EEG. *Epilepsia.* 2009; 50(2):290–296. [PubMed: 18801034]
82. Jozwiak S, Kotulska K, Domanska-Pakiela D, et al. Antiepileptic treatment before the onset of seizures reduces epilepsy severity and risk of mental retardation in infants with tuberous sclerosis complex. *Eur J Paediatr Neurol.* 2011; 15(5):424–431. Suggests that treatment of patients with tuberous sclerosis complex and certain EEG patterns before onset of infantile spasms improves neurological outcome. [PubMed: 21507691]
83. Bombardieri R, Pinci M, Moavero R, Cerminara C, Curatolo P. Early control of seizures improves long-term outcome in children with tuberous sclerosis complex. *Eur J Paediatr Neurol.* 2010; 14(2):146–149. [PubMed: 19369101]

84. Otte WM, van Eijsden P, Sander JW, Duncan JS, Dijkhuizen RM, Braun KP. A meta-analysis of white matter changes in temporal lobe epilepsy as studied with diffusion tensor imaging. *Epilepsia*. 2012; 53(4):659–667. [PubMed: 22379949]
85. Chandra PS, Salamon N, Huang J, et al. FDG-PET/MRI coregistration and diffusion-tensor imaging distinguish epileptogenic tubers and cortex in patients with tuberous sclerosis complex: a preliminary report. *Epilepsia*. 2006; 47(9):1543–1549. [PubMed: 16981871]
86. Gallagher A, Chu-Shore CJ, Montenegro MA, et al. Associations between electroencephalographic and magnetic resonance imaging findings in tuberous sclerosis complex. *Epilepsy Res*. 2009; 87(2–3):197–202. [PubMed: 19783123]
87. Koh S, Jayakar P, Dunoyer C, et al. Epilepsy surgery in children with tuberous sclerosis complex: presurgical evaluation and outcome. *Epilepsia*. 2000; 41(9):1206–1213. [PubMed: 10999561]
88. Mohamed AR, Bailey CA, Freeman JL, Maixner W, Jackson GD, Harvey AS. Intrinsic epileptogenicity of cortical tubers revealed by intracranial EEG monitoring. *Neurology*. 2012; 79(23):2249–2257. [PubMed: 23175730]
89. Major P, Rakowski S, Simon MV, et al. Are cortical tubers epileptogenic? Evidence from electrocorticography. *Epilepsia*. 2009; 50(1):147–154. [PubMed: 19125835]
90. Ma TS, Elliott RE, Ruppe V, et al. Electrocorticographic evidence of perituberal cortex epileptogenicity in tuberous sclerosis complex. *J Neurosurg Pediatr*. 2012; 10(5):376–382. [PubMed: 22998031]
91. Jansen FE, van Huffelen AC, Algra A, van Nieuwenhuizen O. Epilepsy surgery in tuberous sclerosis: a systematic review. *Epilepsia*. 2007; 48(8):1477–1484. [PubMed: 17484753]
92. Mori K, Mori T, Toda Y, et al. Decreased benzodiazepine receptor and increased GABA level in cortical tubers in tuberous sclerosis complex. *Brain Dev*. 2012; 34(6):478–486. [PubMed: 21959128]
93. Jansen FE, van Huffelen AC, Bourez-Swart M, van Nieuwenhuizen O. Consistent localization of interictal epileptiform activity on EEGs of patients with tuberous sclerosis complex. *Epilepsia*. 2005; 46(3):415–419. [PubMed: 15730539]
94. Jambaque I, Cusmai R, Curatolo P, Cortesi F, Perrot C, Dulac O. Neuropsychological aspects of tuberous sclerosis in relation to epilepsy and MRI findings. *Dev Med Child Neurol*. 1991; 33(8):698–705. [PubMed: 1916024]
95. Ridler K, Suckling J, Higgins N, Bolton P, Bullmore E. Standardized whole brain mapping of tubers and subependymal nodules in tuberous sclerosis complex. *J Child Neurol*. 2004; 19(9):658–665. [PubMed: 15563011]
96. Ertan G, Arulrajah S, Tekes A, Jordan L, Huisman TA. Cerebellar abnormality in children and young adults with tuberous sclerosis complex: MR and diffusion weighted imaging findings. *J Neuroradiol*. 2010; 37(4):231–238. [PubMed: 20381146]
97. Asano E, Chugani DC, Muzik O, et al. Autism in tuberous sclerosis complex is related to both cortical and subcortical dysfunction. *Neurology*. 2001; 57(7):1269–1277. [PubMed: 11591847]
98. Tsai PT, Hull C, Chu Y, et al. Autistic-like behaviour and cerebellar dysfunction in Purkinje cell *Tsc1* mutant mice. *Nature*. 2012; 488(7413):647–651. Mouse model with cerebellar injury from *Tsc1* mutations displays autistic behaviors. [PubMed: 22763451]
99. van Eeghen AM, Pulsifer MB, Merker VL, et al. Understanding relationships between autism, intelligence, and epilepsy: a cross-disorder approach. *Dev Med Child Neurol*. 2013; 55(2):146–153. [PubMed: 23205844]
100. Keller TA, Kana RK, Just MA. A developmental study of the structural integrity of white matter in autism. *Neuroreport*. 2007; 18(1):23–27. [PubMed: 17259855]
101. Alexander AL, Lee JE, Lazar M, et al. Diffusion tensor imaging of the corpus callosum in autism. *Neuroimage*. 2007; 34(1):61–73. [PubMed: 17023185]
102. Fletcher PT, Whitaker RT, Tao R, et al. Microstructural connectivity of the arcuate fasciculus in adolescents with high-functioning autism. *Neuroimage*. 2010; 51(3):1117–1125. [PubMed: 20132894]
103. Travers BG, Adluru N, Ennis C, et al. Diffusion tensor imaging in autism spectrum disorder: a review. *Autism Res*. 2012; 5(5):289–313. [PubMed: 22786754]

104. Geschwind DH, Levitt P. Autism spectrum disorders: developmental disconnection syndromes. *Curr Opin Neurobiol.* 2007; 17(1):103–111. [PubMed: 17275283]
105. Peters JM, Taquet M, Vega C, et al. Brain functional networks in syndromic and non-syndromic autism: a graph theoretical study of EEG connectivity. *BMC Med.* 2013; 11(1):54. EEG study that found similar abnormalities in functional connectivity in nonsyndromic (idiopathic) and syndromic (tuberous sclerosis complex) autism, suggesting common biological mechanisms. [PubMed: 23445896]
106. Tuch DS, Reese TG, Wiegell MR, Makris N, Belliveau JW, Wedeen VJ. High angular resolution diffusion imaging reveals intravoxel white matter fiber heterogeneity. *Magn Reson Med.* 2002; 48(4):577–582. [PubMed: 12353272]
107. Taquet M, Scherrer B, Commowick O, et al. Registration and analysis of white matter group differences with a multi-fiber model. *Med Image Comput Comput Assist Interv.* 2012; 15(Pt 3): 313–320. [PubMed: 23286145]
108. Scherrer B, Warfield SK. Parametric representation of multiple white matter fascicles from cube and sphere diffusion MRI. *PLoS ONE.* 2012; 7(11):e48232. [PubMed: 23189128]
109. Taquet M, Scherrer B, Boumal M, Macq B, Warfield SK. Estimation of a multi-fascicle model from single b-value data with a population-informed prior. *Med Image Comput Comput Assist Interv.* 2013 In Press. First study to demonstrate that estimation of multiple fascicles is possible with routine, short acquisition schemes and a single b-value.
110. Scherrer B, Taquet M, Warfield SK. Reliable selection of the number of fascicles in diffusion images by estimation of the generalization error. *Inf Process Med Imaging.* 2013; 7917:742–753.
111. Pasternak O, Westin CF, Bouix S, et al. Excessive extracellular volume reveals a neurodegenerative pattern in schizophrenia onset. *J Neurosci.* 2012; 32(48):17365–17372. [PubMed: 23197727]
112. Wang Y, Wang Q, Haldar JP, et al. Quantification of increased cellularity during inflammatory demyelination. *Brain.* 2011; 134(Pt 12):3590–3601. [PubMed: 22171354]
113. Kwiatkowski DJ, Manning BD. Tuberous sclerosis: a GAP at the crossroads of multiple signaling pathways. *Hum Mol Genet.* 2005; 14(Spec No 2):R251–R258. [PubMed: 16244323]
114. Wullschleger S, Loewith R, Hall MN. TOR signaling in growth and metabolism. *Cell.* 2006; 124(3):471–484. [PubMed: 16469695]
115. Sahin M. Targeted treatment trials for tuberous sclerosis and autism: no longer a dream. *Curr Opin Neurobiol.* 2012; 22:1–7. [PubMed: 22305967]
116. Franz DN, Belousova E, Sparagana S, et al. Efficacy and safety of everolimus for subependymal giant cell astrocytomas associated with tuberous sclerosis complex (EXIST-1): a multicentre, randomised, placebo-controlled Phase 3 trial. *Lancet.* 2012; 381(9861):125–132. [PubMed: 23158522]
117. Kotulska K, Chmielewski D, Borkowska J, et al. Long-term effect of everolimus on epilepsy and growth in children under 3 years of age treated for subependymal giant cell astrocytoma associated with tuberous sclerosis complex. *Eur J Paediatr Neurol.* 2013 Epub ahead of print. 10.1016/j.ejpn.2013.03.002
118. Meikle L, Pollizzi K, Egnor A, et al. Response of a neuronal model of tuberous sclerosis to mammalian target of rapamycin (mTOR) inhibitors: effects on mTORC1 and Akt signaling lead to improved survival and function. *J Neurosci.* 2008; 28(21):5422–5432. [PubMed: 18495876]
119. Zeng LH, Xu L, Gutmann DH, Wong M. Rapamycin prevents epilepsy in a mouse model of tuberous sclerosis complex. *Ann Neurol.* 2008; 63(4):444–453. [PubMed: 18389497]
120. Wong M. Mammalian target of rapamycin (mTOR) inhibition as a potential antiepileptogenic therapy: from tuberous sclerosis to common acquired epilepsies. *Epilepsia.* 2010; 51(1):27–36. [PubMed: 19817806]
121. Ehninger D, Han S, Shilyansky C, et al. Reversal of learning deficits in a *Tsc2<sup>+/-</sup>* mouse model of tuberous sclerosis. *Nat Med.* 2008; 14(8):843–848. [PubMed: 18568033]
122. Wakana S, Caprihan A, Panzenboeck MM, et al. Reproducibility of quantitative tractography methods applied to cerebral white matter. *Neuroimage.* 2007; 36(3):630–644. [PubMed: 17481925]

201. Roberds, S. [Accessed 1 July 2013] Diagnostic criteria. Tuberous Sclerosis Alliance. How is TSC diagnosed?. 2013. [www.tsalliance.org/pages.aspx?content=10](http://www.tsalliance.org/pages.aspx?content=10)

## Executive summary

### **Tuberous sclerosis complex is a multiorgan disorder with an unpredictable phenotype**

- Neurologically, tuberous sclerosis complex (TSC) is associated with epilepsy, intellectual disability and autism spectrum disorder.
- Neither genotype nor any conventional imaging biomarker is a reliable and sufficient predictor for neurological outcome.

### **Diffusion tensor imaging is a modeling method of tissue water diffusion**

- Water diffusion can be quantified by two main diffusion tensor imaging (DTI) measures: fractional anisotropy, which reflects degree of preferential directionality of diffusion, and mean diffusivity, which is an average of diffusion in all directions.
- Tractography is based on lining up diffusion tensors, prolate (cucumber) shapes, with the longest axis reflecting preferential diffusion. These tracts accurately reflect the anatomy of major white matter pathways in humans.

### **In TSC, DTI measures correlate with pathology & clinical phenotype**

- Microstructural tissue properties, as measured by DTI, correspond to abnormalities in myelination, axonal organization, altered extracellular milieu and possibly to aberrations in axonal, dendritic and synaptic development and function. However, small-animal MRI with DTI of TSC mouse models is required to confirm these relationships.
- DTI can assist with localization of epileptogenic tubers, confirmed by neurophysiological and other imaging modalities, potentially affecting neurosurgical outcome of epilepsy surgery in TSC.
- DTI abnormalities of the normal-appearing white matter are associated with the presence of autism spectrum disorder in TSC.

### **mTOR inhibitors that target the molecular deficit in TSC are showing promise with regard to multiple neurological symptoms**

- mTOR inhibitors (mTOR-is) reduce subependymal giant-cell astrocytoma in both adults and children with TSC.
- mTOR-is have shown anti-epileptic and, potentially, anti-epileptogenic effects in mouse models.
- mTOR-is may improve cognition and behavior, potentially opening avenues for early pharmacological treatment of autism in TSC.
- Whether DTI can become an industry-standard biomarker for mTOR-related treatment changes in TSC remains to be investigated.

### **Conclusion**

- There is unprecedented and dramatic progress in the field of TSC, first with the emergent use of mTOR-is for seizures, cognition and potentially autism, and second with DTI as a candidate biomarker for cognitive and behavioral outcome.
- If DTI proves to be a reliable and biologically meaningful biomarker for patient stratification and treatment response, clinical trials will be much facilitated.



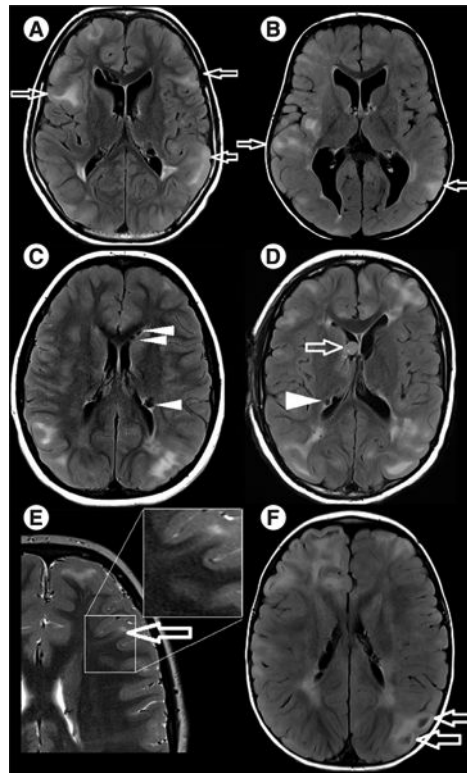


**Figure 1. Conventional MRI findings in tuberous sclerosis complex**

(A & B) Axial fluid attenuation inversion recovery images. Both patients have subcortical tubers (arrows) of comparable size and distribution (not all tubers shown in current plane), but patient (A) has severe autism, no active seizure disorder and is nonverbal, while patient (B) has mild motor and language delays, no autism and refractory seizures despite multiple antiepileptic drugs. (C & D) Axial fluid attenuation inversion recovery images. Hypointense partially calcified subependymal nodules are seen lining the ependyma (arrowheads) and a subependymal giant cell astrocytoma is seen in (D), at the level of the foramen of Monro (arrow). (E) Axial T2-weighted image shows a radial migration line tracking from the tuber into the deep white matter (arrow, and zoom frame). (F) Axial fluid attenuation inversion recovery image. Cyst-like appearance of a tuber (arrows).

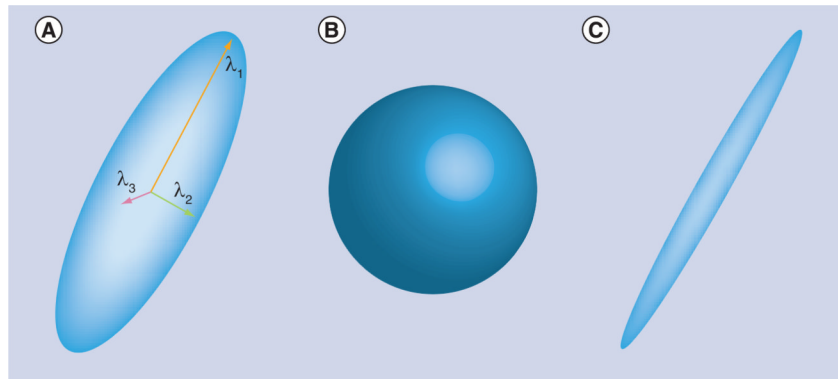


**Figure 2. Diffusion tensor imaging is the most common model of the diffusion**

(A) Diffusion tensor imaging can be represented as an ellipsoid that consists of three axes of diffusion and the corresponding diffusivities (here  $\lambda_1$ ,  $\lambda_2$  and  $\lambda_3$ ). The shape of the ellipsoids provides information about the type of diffusion present in the voxel. (B) An isotropic diffusion leads to a spherical tensor. (C) Diffusion that is highly restricted in two directions and favored in one direction will present as an elongated tensor with very small second and third diffusivities.

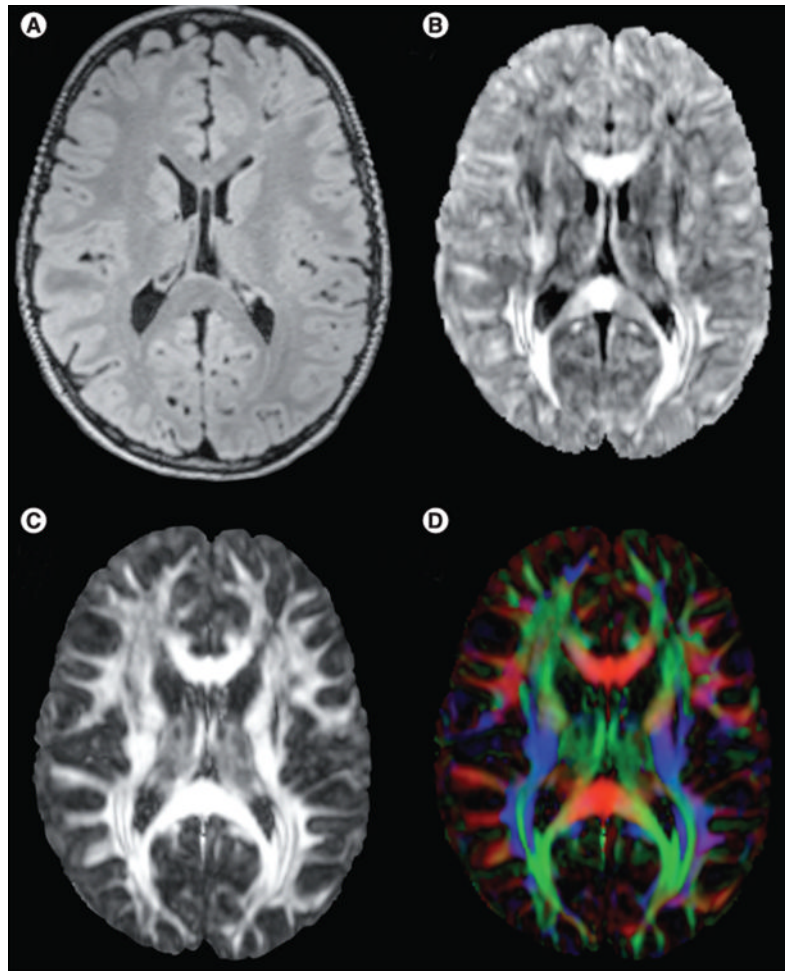


**Figure 3. Diffusion tensor imaging and diffusion tensor imaging-based measures**  
 (A) Fluid attenuation inversion recovery MRI structural image, axial plane. (B) Mean diffusivity image. Mean diffusivity is especially large in the corpus callosum and in corticospinal tracts. (C) Fractional anisotropy (FA) image shows where in the brain diffusion is more (white) or less (black) anisotropic. Owing to the presence of highly structured white matter fascicles with aligned axons and myelin sheath, FA in the white matter is high. By contrast, gray matter present in axons with various directions, results in a lower FA. (D) FA can be colored based on the directions of the fascicle in each voxel: red means the fascicle is oriented left to right, green represents fascicles that are oriented along the anterior–posterior axis and blue represents the superior–inferior axis. For color images please see [www.futuremedicine.com/doi/pdf/10.2217/fnl.13.37](http://www.futuremedicine.com/doi/pdf/10.2217/fnl.13.37).

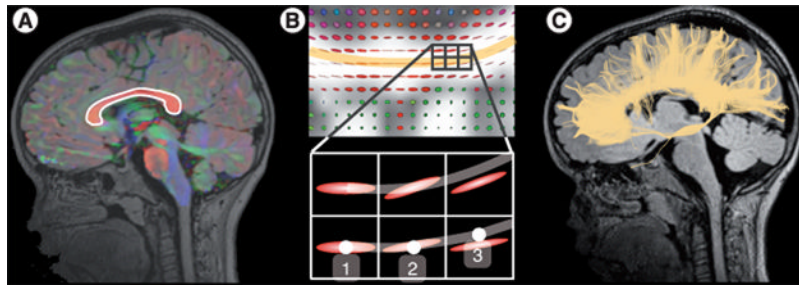


**Figure 4. Tractography allows detection of white matter pathways in the brain**

(A) A seeding region is first defined (here the corpus callosum) from where tracts will start growing. (B) From each voxel of the seeding region, tracts grow in the direction of the tensor. (C) Step by step, from voxel to voxel, tracts keep growing until they reach the gray matter where they stop. This yields 3D maps of the fascicles in the brain, all connected to the seeding region. In order to avoid spurious fibers when performing tractography, using two seed points instead of one can be more accurate [122]. A correction for the density of tracts can also be applied, in which spurious tracts get largely ignored in calculating an average of a diffusion metric [23].

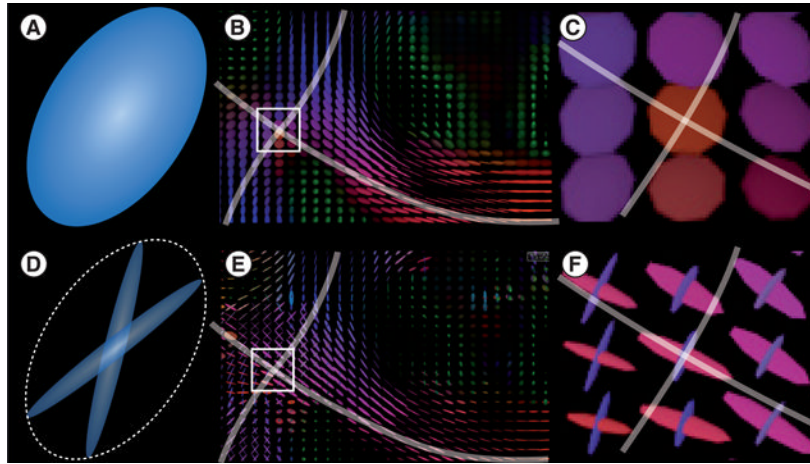


**Figure 5. Single tensor and multifascicle models**

(A–C) Unlike assumptions of the diffusion tensor models, fascicles in the voxels may have more than one preferential direction. Diffusion tensor imaging model assumes that a single fascicle is present at each voxel. This assumption is violated in regions where fascicles cross, such as (B) the corona radiata. In those regions, tensors are abnormally inflated to capture the signal arising from (C) each fascicle, resulting in a lower fractional anisotropy that may be misleadingly interpreted. (D–F) By contrast, multifascicle models represent each fascicle independently and are, therefore, able to characterize regions with crossing fascicles.

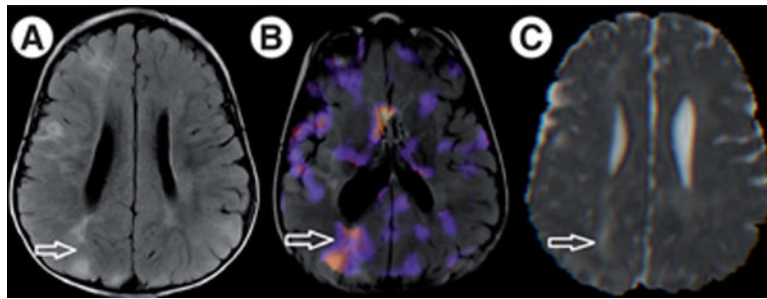


**Figure 6. A 2-year-old patient with tuberous sclerosis complex with an epileptogenic right parietal tuber**

Visible on (A) axial fluid attenuation inversion recovery image, arrow indicates large right parietal tuber. (B) Single-photon emission CT scan with an injection shortly after onset of a seizure, demonstrating focal increased tracer uptake in the epileptogenic tuber (note the difference in angulation of the image). (C) Mean diffusivity image, revealing elevated mean diffusivity ( $0.0015 \text{ mm}^2/\text{s}$ ) at the tuber compared with elsewhere in white matter ( $0.0008 \text{ mm}^2/\text{s}$ ). The tuber was resected and the patient has been seizure-free for over 6 months.



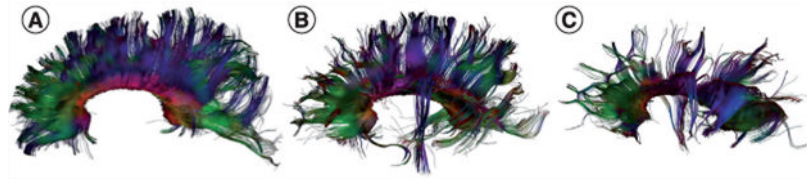


**Figure 7. Diffusion tensor imaging of the corpus callosum in tuberous sclerosis complex** (A–C) Tractography renderings of the corpus callosum of three subjects: (A) healthy control, mean fractional anisotropy (FA) is 0.46; (B) patient with tuberous sclerosis complex, no autism spectrum disorder, mean FA is 0.50; and (C) patient with tuberous sclerosis complex and autism spectrum disorder, mean FA is 0.34. The corpus callosum of (B) and (C) are more ragged owing to tubers interfering with streamlines, but only in the patient with autism spectrum disorder is the mean FA is lower. (C) Reproduced with permission from [23].